INTERNATIONAL JOURNAL OF CLIMATOLOGY
Int. J. Climatol. (2014)
Published online in Wiley Online Library
(wileyonlinelibrary.com) DOI: 10.1002/joc.3939

Observation of spatial patterns on the rainfall response to ENSO and IOD over Indonesia using TRMM Multisatellite Precipitation Analysis (TMPA)

Abd. Rahman As-syakur,[a,b]* I Wayan Sandi Adnyana,[c] Made Sudiana Mahendra,[b] I Wayan Arthana,[d] I Nyoman Merit,[c] I Wayan Kasa,[e] Ni Wayan Ekayanti,[a,f] I Wayan Nuarsa[b] and I Nyoman Sunarta[g]

[a] *Center for Remote Sensing and Ocean Science (CReSOS), Udayana University, Bali, Indonesia*
[b] *Environmental Research Center (PPLH), Udayana University, Bali, Indonesia*
[c] *Faculty of Agriculture, Udayana University, Bali, Indonesia*
[d] *Faculty of Oceanography and Fisheries, Udayana University, Bali, Indonesia*
[e] *Faculty of Science, Udayana University, Bali, Indonesia*
[f] *Physic Department, Technical High School of Tampaksiring, Bali, Indonesia*
[g] *Faculty of Tourism, Udayana University, Bali, Indonesia*

ABSTRACT: Remote sensing data of Tropical Rainfall Measuring Mission (TRMM) Multisatellite Precipitation Analysis for 13 years have been used to observe the spatial patterns relationship of rainfall with El Niño-Southern Oscillation (ENSO) and Indian Ocean Dipole (IOD) over Indonesia. Linear correlation was measured to determine the relationship level by the restriction analysis of seasonal and monthly relationship, while the partial correlation technique was utilized to distinguish the impact of one phenomenon from that of the other. Application of remote sensing data can reveal an interaction of spatial-temporal relationship of rainfall with ENSO and IOD between land and sea. In general, the temporal patterns relationship of rainfall with ENSO confirmed fairly similar temporal patterns between rainfall with IOD, which is high response during JJA (June–July–August) and SON (September–October–November) and unclear response during DJF (December–January–February) and MAM (March–April–May). Spatial patterns relationship of both phenomena with rainfall is high in the southeastern part of Sumatra Island and Java Island during JJA and SON. During the SON season, IOD has a higher relationship level than ENSO in this part. In the spatial-temporal pattern seen, a dynamic movement of the relationship between IOD and ENSO with rainfall in Indonesia is indicated, where the influence of ENSO and IOD started during JJA especially in July in the southwest of Indonesia and ended in the DJF period especially in January in the northeast of Indonesia.

KEY WORDS rainfall; remote sensing; ENSO; IOD; TMPA; partial correlation

Received 23 March 2011; Revised 29 November 2013; Accepted 7 January 2014

1. Introduction

Indonesia is an equator-crossed country surrounded by two oceans and two continents. This location makes Indonesia a region of confluence of the Hadley cell circulation and the Walker circulation, two circulations that greatly affect the diversity of rainfall in Indonesia (Aldrian *et al.*, 2007). The annual movement of the sun from 23.5°N to 23.5°S produces the monsoon activity, and it also plays a role in influencing the diversity of the rainfall. Local influence of rainfall variability also cannot be ignored because Indonesia is an archipelago with a varied topography (Haylock and McBride, 2001; Aldrian and Djamil, 2008). On the other hand, complex distribution of land and sea results in significant local variations in the annual rainfall cycle (Chang *et al.*, 2005; Qian, 2008), and affects the rainfall quantities (Sobel *et al.*, 2011; As-syakur *et al.*, 2013). Furthermore, the differential solar heating between different surface types such as between land and sea, or highland and lowland, causes strong local pressure gradients (Qian, 2008). These conditions result in sea-breeze convergence over islands and orographic precipitation (Qian *et al.*, 2010), causing diurnal cycle of rainfall over islands. Overall, rain is the most important climate element in Indonesia because precipitation varies both with respect to time and space. Therefore, this study about climate in Indonesia focused more on the rain factor.

Atmosphere–ocean interactions near Indonesia such as the El Niño-Southern Oscillation (ENSO) and the Indian Ocean Dipole (IOD) mode also contribute to the inter-annual climate variations. Both the climate modes are important because of their large environmental and societal impacts, globally and regionally (Luo *et al.*, 2010).

* Correspondence to: A. R. As-syakur, Center for Remote Sensing and Ocean Science (CReSOS), Udayana University, Bali 80232, Indonesia.
E-mail: ar.assyakur@pplh.unud.ac.id

Indonesian rainfall is coherent and strongly correlated with ENSO variations in the Pacific basin (Ropelewski and Halpert, 1987; Nicholls, 1988; Aldrian and Susanto, 2003; Hendon, 2003; Aldrian *et al.*, 2007; Hamada *et al.*, 2012) and also correlated with IOD events (Saji *et al.*, 1999; Saji and Yamagata, 2003b; Bannu *et al.*, 2005). ENSO is a recurring pattern of climate variability in the eastern equatorial Pacific, which is characterized by anomalies in both sea surface temperature (SST; referred to as El Niño and La Niña for warming and cooling periods, respectively) and sea-level pressure (Southern Oscillation; Philander, 1990; Trenberth, 1997; Naylor *et al.*, 2001; Meyers *et al.*, 2007). An IOD event refers to strong zonal SST gradients in the equatorial Indian Ocean regions, phase-locked to the boreal summer and autumn (Saji *et al.*, 1999; Saji and Yamagata, 2003a, 2003b).

Moreover, Indonesian rainfall is also influenced by intra-seasonal (30–90 days) Madden–Julian oscillation (MJO; e.g. Madden and Julian, 1971), a dominant component of intra-seasonal variability over the Tropics (Wheeler and Hendon, 2004). Large-scale tropical convection–circulation phase of MJO significantly affects the rainfall variability over Indonesia (Hidayat and Kizu, 2010; Oh *et al.*, 2012). Extreme high and low precipitation events were associated with the MJO phase and causes floods and droughts in some places of Indonesia. However, spatial characteristics and manifestations of MJO are affected and modified by the ENSO and IOD conditions (Hendon *et al.*, 2007; Rao *et al.*, 2007; Tang and Yu, 2008; Waliser *et al.*, 2012). During El Niño, the number of intra-seasonal days decreases and the opposite tends to occur in the La Niña event (Pohl and Matthews, 2007). On the other hand, during negative IOD, the MJO propagation is slightly stronger than normal and relatively weak during positive IOD (Wilson *et al.*, 2013).

El Niño (La Niña) conditions result in a decrease (enhance) in rainfall in Indonesia (Ropelewski and Halpert, 1987; Philander, 1990; Hendon, 2003; Bannu *et al.*, 2005; Susilo *et al.*, 2013); on the other hand, positive (negative) IOD is also decreasing (enhancing) the rainfall in Indonesia (Saji *et al.*, 1999; Saji and Yamagata, 2003b; Bannu *et al.*, 2005; Aldrian *et al.*, 2007). Decrease in rainfall during El Niño and positive IOD resulted in longer dry season than the normal conditions (Philander, 1990; Saji *et al.*, 1999; Hamada *et al.*, 2002; Hendon, 2003). On the other hand, the La Niña event creates wet condition during the dry season and also increases rainfall at the beginning of the rainy season (Bell *et al.*, 1999, 2000; Hendon, 2003), which creates a high risk of flood (Kishore and Subbiah, 2002). Meanwhile, in El Niño and positive IOD-related rainfall deficits, significantly below-normal rainfall from June through December resulted in extreme drought that contributes to large forest and peat fires, air pollution and haze from biomass burning (Bell and Halpert, 1998; Gutman *et al.*, 2000; Waple and Lawrimore, 2003; Chrastansky and Rotstayn, 2012) and causes extreme low streamflow in basins (Sahu *et al.*, 2012); at the same time, El Niño and positive IOD also influence a decline in crop productivity (Irawan, 2003; D'Arrigoa and Wilson, 2008).

Precipitation displays high space–time variability that requires frequent observations for adequate representation (Hong *et al.*, 2010). Previous estimates of tropical precipitation were usually made on the basis of climate prediction models and the occasional inclusion of very sparse surface rain gauges and/or relatively few measurements from satellite sensors (Feidas, 2010). Rain gauge observations yield relatively accurate point measurements of precipitation but suffer from sampling errors in representing areal means and are not available over most oceanic and unpopulated land areas (Xie and Arkin, 1996; Petty and Krajewski, 1996). However, nowadays, rainfall data required for a wide range of scientific applications can be achieved through meteorological satellites (Petty, 1995). Meteorological satellites expand the coverage and time span of conventional ground-based rainfall data for a number of applications by which all hydrology and weather forecasting are made (Levizzani *et al.*, 2002). Furthermore, combining information from multiple satellite sensors as well as gauge observations and numerical model outputs yields analyses of global precipitation with stable and improved quality (Xie *et al.*, 2007). In Indonesia, precipitation is represented as rain gauge data throughout the country. However, rain gauges have incomplete coverage over remote and undeveloped land areas and particularly over the sea, where such instruments are virtually not available. Data that have better spatial-temporal resolutions of rainfall will allow a more quantitative understanding of the causal links of Indonesian rainfall to larger scale climate features. The use of remote sensing, which has better spatial and temporal resolution data, in a study about rainfall and its spatial relationship to ENSO and IOD in Indonesia, thus offers an exciting opportunity.

Tropical Rainfall Measuring Mission (TRMM) Multisatellite Precipitation Analysis (TMPA) products, often called combined or merged analyses, have been utilized in a wide range of applications, including weather/climate monitoring, climate analysis, numerical model verifications, and hydrological studies (Xie *et al.*, 2007). The TMPA rain products are based on TRMM Precipitation Radar (PR) and TRMM Microwave Imager (TMI) combined rain rates to calibrate rain estimates from other microwave and infrared (IR) measurements (Huffman *et al.*, 2007). The TMPA product is more suitable for this study because the available rain gauge measurements are also used in the calibration process (Mehta and Yang, 2008). For many years, other groups have studied different locations to validate TRMM 3B43 data. For example, Semire *et al.* (2012) validated TRMM 3B43 rainfall for Malaysia, As-syakur *et al.* (2011) compared the TMPA with rain gauge data in Bali, Fleming *et al.* (2011) evaluated the TRMM 3B43 using gridded rain-gauge data over Australia, Chokngamwong and Chiu (2008) compared the TMPA with rain gauge data in Thailand, and Islam and Uyeda (2007) validated TRMM 3B43 and

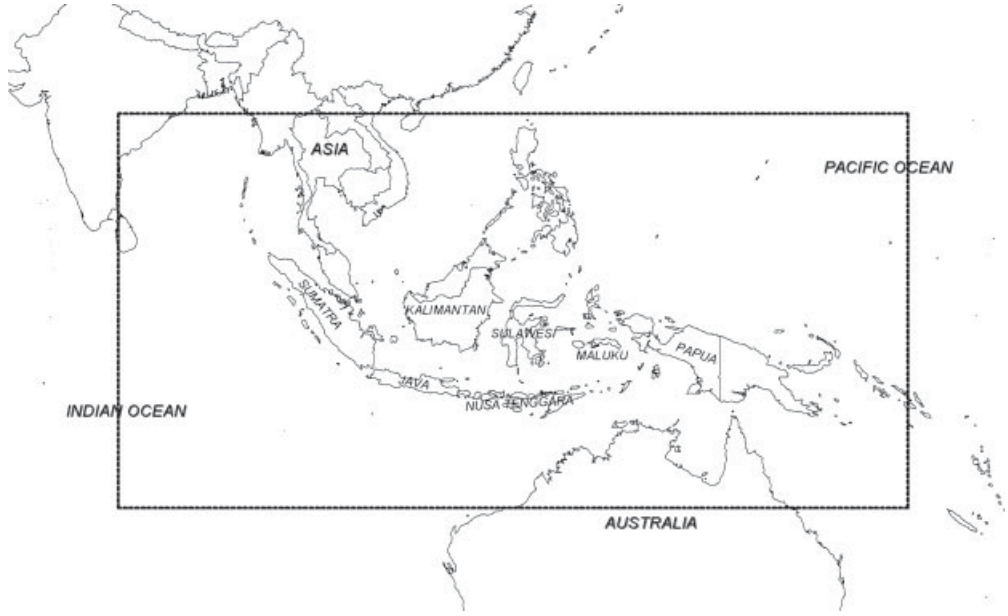

Figure 1. Spatial cover of research.

determined the climatic characteristics of rainfall over Bangladesh. On the other hand, Vernimmen *et al.* (2012) and Prasetia *et al.* (2013) have validated for other types of TRMM in Indonesia. Vernimmen *et al.* (2012) compared and used real-time TRMM 3B42 to monitor drought in Indonesia, and Prasetia *et al.* (2013) validated TRMM PR over Indonesia. The results have underscored the superiority of the TMPA or TRMM 3B43 product and the goal of the algorithm has been achieved to a large extent. Nonetheless, the satellite data display a few drawbacks for tropical regions as bias error against ground base *in situ* observation. Limitations of the TRMM are that the data are affected by several factors such as causes of non-Sun-synchronous satellite orbit, narrow swath of satellite data, rainfall types (convective and stratiform), and insufficient sampling time intervals, which result in loss of information about rainfall values (Fleming *et al.*, 2011; Vernimmen *et al.*, 2012; As-syakur *et al.*, 2013; Prasetia *et al.*, 2013).

Based on these conditions, in this work we attempt to use the rainfall data from TMPA products to know the spatial patterns relationship of rainfall with ENSO and IOD over Indonesia. Previous studies on the relationship between rainfall with ENSO and IOD in Indonesia were carried out in many locations that have rain gauge data or model utilizations where the data come only from the rain gauge (e.g. Ropelewski and Halpert, 1987; Nicholls, 1988; Hamada *et al.*, 2002; Hendon, 2003; Saji and Yamagata, 2003b; Aldrian *et al.*, 2007). So with the existence of satellite data that have a better spatial-temporal resolution, useful information about the spatial patterns relationship between rainfalls with both types of index can be expected. In this study, the ENSO condition is defined by the Southern Oscillation Index (SOI; Ropelewski and Jones, 1987; Ropelewski and Halpert, 1989, 1996; Können *et al.*, 1998; Hamada *et al.*, 2002), and the IOD condition is defined by Dipole Mode Index (DMI) values (Saji *et al.*, 1999; Saji and Yamagata, 2003a, 2003b). Main analyses are carried out by using seasonal and monthly spatial correlations.

2. Data and Methods

2.1. Data

Monthly rainfall data from 1998 to 2010, which were measured and collected by TMPA, were used to analyse the spatial patterns relationship between rainfall with ENSO and IOD. Cover spatial data used in this research are 20°N to 20°S and 80°E to 160°E (Figure 1) with as much as 51,200 TMPA pixels being analysed. SOI values were used to determine warm (El Niño) and cold (La Niña) events in the Pacific Ocean (Ropelewski and Jones, 1987; Ropelewski and Halpert, 1989; Können *et al.*, 1998). Meanwhile, DMI values are used to determine positive IOD and negative IOD events in the Indian Ocean (Saji *et al.*, 1999; Saji and Yamagata, 2003a, 2003b). The SOI can be considered as the atmospheric manifestation of the ENSO (McBride *et al.*, 2003), meanwhile the DMI can be considered as a manifestation of the IOD (Saji *et al.*, 1999; Saji and Yamagata, 2003b). SOI is an index that is based on the difference in the pressure data between Tahiti and Darwin (Ropelewski and Jones, 1987) and is defined as the standardized difference between the standardized monthly pressures at Tahiti and Darwin (Können *et al.*, 1998), whereas the DMI is defined as the SST gradient between the eastern and western tropical Indian Ocean (Saji *et al.*, 1999). In previous studies, it was found that SOI values have a high correlation with Indonesian rainfall (e.g. Ropelewski and Jones, 1987; Ropelewski and Halpert, 1989, 1996; Hamada *et al.*, 2002; Haylock and McBride, 2001; McBride *et al.*,

2003), as well as DMI values (e.g. Saji *et al.*, 1999; Saji and Yamagata, 2003b; Bannu *et al.*, 2005).

The TRMM is cosponsored by the National Aeronautics and Space Administration (NASA) of the United States, and the Japan Aerospace Exploration Agency (JAXA, previously known as the National Space Development Agency, or NASDA) has collected the data since November 1997 (Kummerow *et al.*, 2000). TRMM is a long-term research programme designed to study the Earth's land, oceans, air, ice, and life as a total system (Islam and Uyeda, 2007). TMPA is a calibration-based sequential scheme for combining precipitation estimates from multiple satellites, gauge analyses where feasible, as well as providing a global coverage of precipitation above the 50°S–50°N latitude belt at $0.25^{\circ} \times 0.25^{\circ}$ spatial and 3-hourly temporal resolutions for 3B42 and monthly temporal resolution for 3B43 (Huffman *et al.*, 2007). The TMPA estimates are produced in four stages: (1) the microwave estimates of precipitation are calibrated and combined, (2) infrared precipitation estimates are created using the calibrated microwave precipitation, (3) the microwave and infrared estimates are combined, and (4) rescaling to monthly data is applied (Huffman *et al.*, 2007, 2010). The TMPA retrieval algorithm used for this product is based on the technique by Huffman *et al.* (1995, 1997) and Huffman (1997). In this paper, TMPA data types used are of 3B43 version 6 (V6).

Furthermore, the version 4 (V4) of SST from the TMI is used to determine the environmental factors that affect the spatial-temporal variations of ENSO–rainfall (IOD–rainfall) relations. The inclusion of the 10.7 GHz channel in the TMI provides the additional capability to accurately measure SST through clouds (Wentz *et al.*, 2000).

The TMPA 3B43 V6 can be referred to from the website ftp://disc2.nascom.nasa.gov/data/s4pa/ TRMM_L3/. The SOI and DMI data are obtained from the websites http://www.bom.gov.au/ and http://www.jamstec.go.jp/, respectively. In addition, the V4 of SST data from TMI can be referred to from the website ftp://ftp.ssmi.com/tmi.

2.2. Methods

Statistical score can be used to analyse the relationship of TMPA to the SOI and DMI values. The proximity of the satellite estimates to the index values are measured by the linear correlation coefficient. In the statistical lexicon, the correlation is used to describe a linear statistical relationship between two random variables that vary together precisely, one variable being related to the other by means of a positive (negative) scaling factor (von Storch and Zwiers, 1999). Positive (negative) correlation between rainfall and SOI indicates that the warm event in the Pacific Basin can lead to decreased (increased) rainfall, whereas the opposite tends to occur during the cold event. Meanwhile, negative (positive) correlation between rainfall and DMI indicates that the cold event in the eastern tropical Indian Ocean can lead to decreased (increased) rainfall, whereas the opposite tends to occur during the warm event. Confidence levels of 95% and 99% are used to determine the significance level of correlation.

The main analysis in this research is about the monthly relationship, but similar measures have been applied to the seasonal analysis as well. Analysis carried out in each pixel is with the coordinates as identity. Data extracted from the TMPA in each pixel are used to generate point-by-point data. The point gives the coordinate, month, year, and rainfall values. The data are then sorted in accordance with the purposes of analysis. The same sorting process is also carried out on index values (SOI and DMI), and followed by calculations with the linear correlation. After obtaining the correlation value, the point data is converted into a raster data format that has the same spatial resolution as the original data ($0.25^{\circ} \times 0.25^{\circ}$).

Monthly analysis is carried out by correlating the monthly data of the same month from the yearly observation. Seasonal analysis are carried out based on the monsoon activity, where the seasons are divided into four groups: December–January–February (DJF), March–April–May (MAM), June–July–August (JJA), and September–October–November (SON). DJF represents the peak of the northwest Australia–Asia monsoon, and JJA represented the peak of the southeast Australia–Asia monsoon, while both MAM and SON represent monsoon transitions (Aldrian and Susanto, 2003). Seasonal analysis will be carried out by correlating the monthly data of the same season from the yearly observation.

Indonesian rainfalls are known to be correlated with ENSO and IOD. It is feasible, therefore, that the correlations examined here between rainfall and both indices may not imply a direct relationship but, rather, that the relationship between rainfall and both indices are influenced by one of the two indices that has an independent correlation. To address the problem of multiple drivers, partial correlation is commonly used. Partial correlation is a technique used to measure the correlation between two related variables after eliminating the influence of one or more other variables, or, on the supposition that the other variables become constants (Blair, 1918). Correlation between two variables may occur because both of them are correlated with a third variable or a set of variables (Cramer, 2003). Partial correlation controls for this possible correlation with a third identified variable or a set of variables (Delbanco *et al.*, 1998). Conversely, the method may unduly penalize the original driver, as the part of the original driver that is correlated with the second driver might still reflect the operation of the original driver. Partial correlation method has been applied to determine the impacts of ENSO and IOD events, such as on sub-regional Indian summer monsoon rainfall (Ashok and Saji, 2007), on Australian rainfall (Cai *et al.*, 2011), and on winter storm-track activity over the Southern Hemisphere (Ashok *et al.*, 2007). For the three rainfall quantities, the partial coefficient is given by the equation

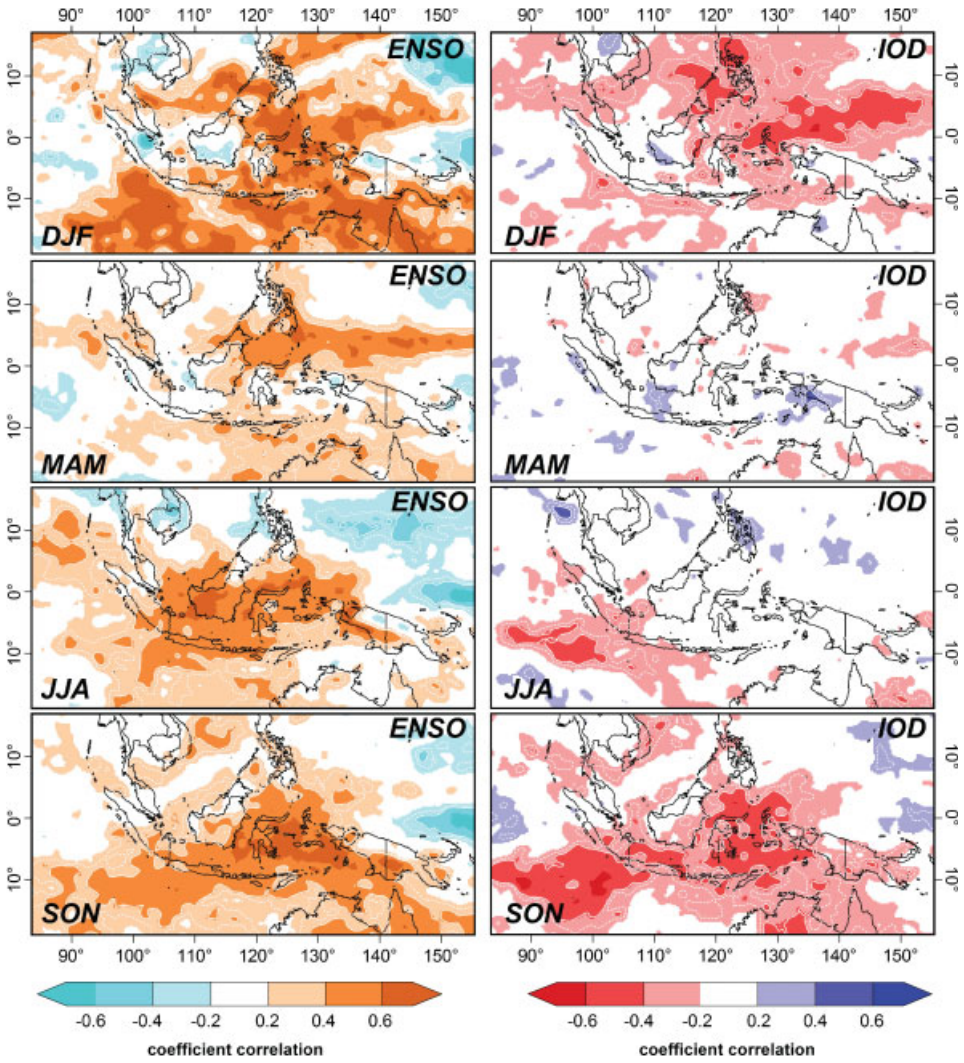

Figure 2. Spatial patterns seasonal analysis of the relationship between rainfall with ENSO and IOD. White dashed line and solid line indicate significant level of correlation under 95% and 99%, respectively.

(Blair, 1918):

$$r_{12,3} = \frac{r_{12} - r_{13}r_{23}}{\sqrt{\left(1 - r_{13}^2\right)\left(1 - r_{23}^2\right)}}, \qquad (1)$$

where $r_{12,3}$ is the partial correlation between two random variables, 1 and 2, after removing the controlling effect of another random variable, 3. When the effect of IOD is removed, variables 1, 2, and 3 can be taken as rainfall, the SOI, and the DMI, respectively. In addition, if we reverse the roles of 2 and 3, $r_{12,3}$ would become a measure of the rainfall related to the IOD and the effect of ENSO is removed. In case the effect of IOD is removed, r_{12} and r_{13} are the simple correlations between rainfall and SOI, and rainfall and DMI, respectively. The opposite effect results when ENSO is removed. When the effect of IOD is removed, the square of the quantity, $r_{12,3}$, answers the question of how much of the rainfall variance that is not estimated by IOD in the equation is estimated by ENSO, whereas the opposite tends to occur when the effect of ENSO is removed.

3. Results

3.1. Seasonal analysis

The seasonal spatial patterns relationship between rainfall with ENSO and IOD is presented in Figure 2. During DJF season, SOI fluctuation (describe by positive correlation) influences the occurrence of rainfall in the western part of Indonesia although the distribution is not smooth. The area affected by ENSO are part of Java Sea, part of Nusa Tenggara island, part of northeast Sulawesi island, part of Maluku Islands, and a small part of Papua. The biggest ENSO effect in rainfall fluctuation in this season is found in the northern and southern sides of Indonesia. The spatial distribution of IOD effect concerning the rainfall fluctuation during DJF season is smaller than that of the ENSO effect. The IOD effect (describe by negative correlation) on rainfall fluctuation is found only in the northern and northeast parts of Indonesia, such as eastern part of Kalimantan, northern part of Sulawesi, northern part of Maluku Islands, and also a small part of Papua. A better condition can be found in MAM season.

During MAM season, ENSO effect is not as wide as other monsoon seasons; moreover, IOD phenomenon has very small effect concerning rainfall in Indonesia. ENSO effect is found only outside Indonesia, e.g. the northern and southern parts of Kalimantan except the eastern area of Kalimantan. Outside of Indonesia, regions affected by the ENSO phenomenon in MAM season are northern part of Sulawesi, northern part of Maluku, southern part of Nusa Tenggara island, and southern part of Papua. During this season, the IOD phenomenon is correlated only with the rainfall in the southern coast of Papua and Maluku Island. Meanwhile, the type of correlation is positive, which means in positive IOD, the rainfall increases.

Spatial patterns responses between rainfall with ENSO and IOD during JJA season can be seen clearly and are clustered. The widest ENSO effect on Indonesian rainfall can be found in JJA season. The rainfall shows insignificant correlation with ENSO in the western part of Sumatra, northeast of Kalimantan and northern part of Papua. Meanwhile, the IOD effect on rainfall fluctuation in Indonesia which is found as a cluster in the southwest of Indonesia is in the small part of southeast of Sumatra and in the western part of Java. During the SON period, the widest spatial distribution of correlation between rainfall with ENSO and IOD in the Indonesian area was found. The ENSO effect has been seen to decrease in the west and move to the eastern part of Indonesia. Relationship between rainfall and ENSO in Kalimantan, Sumatra, and Java islands has smaller correlation compared to JJA season. Meanwhile, Sulawesi and Maluku Island have strong correlation with ENSO. Influence of IOD on rainfall in this season is found to move to the eastern part of Indonesia. Besides the influence of rainfall in the southeast of Sumatra and Java, the IOD effect can also be found in Sulawesi, Nusa Tenggara, Maluku Island, and part of Papua.

Figure 3 shows the seasonal patterns of spatial partial correlation between TMPA rainfall with ENSO when the effect of IOD is removed, and with IOD when the effect of ENSO is removed. Generally, the spatial distributions of the partial correlation between rainfall with ENSO and IOD are similar to the spatial patterns of seasonal linear correlation except in ENSO during the SON season and in IOD during the DJF and SON seasons (compare Figures 2 and 3). Removal of the effects of IOD (ENSO) weakens the positive (negative) correlation with rainfall. However, IOD affects the spatial patterns of ENSO during SON season to reduce the spatial distributions of the ENSO effect. On the other hand, the spatial distributions of IOD are influenced by the ENSO phenomenon in DJF and SON seasons. In DJF season, the spatial patterns of partial correlation between rainfall and IOD are wider than the linear correlation (compare Figures 2(e) and 3(e)) which reduces negative correlation in the northern part of Maluku Island and produces positive correlation in the southeastern part of Indonesia. In SON season, the smallest spatial distribution of partial correlation was found as a cluster in the southwest of Indonesia and was not seen in the mainland of Indonesia.

3.2. Monthly analysis

The second result in this study is the monthly spatial patterns relationship between rainfall and ENSO and IOD, which are presented in Figures 4 and 5. During January, the ENSO and IOD influence is obvious, particularly in the eastern part of Indonesia. In general, during February and June, the influences of both climate phenomena are not that clear in the mainland area. Influence of ENSO during February to May is seen outside the Indonesian archipelago, that is, the southern and northern parts. During February to April, the positive correlation between *rainfall* and ENSO could be seen clustered outside the Indonesian archipelago, that is, the northern part. However, during April to June, the positive correlation value is seen outside of the Indonesian archipelago, that is, the southern part.

Strong response of ENSO during July occurred in the centre part of Indonesia, particularly in Java, Nusa Tenggara, Kalimantan, Sulawesi, and Maluku. On the other hand, a strong response of IOD occurred in the southern part outside of Indonesia, especially in Java. During August, the strong responses of ENSO remain in the centre part of Indonesia, but move slightly to the north (Kalimantan) and move out from Nusa Tenggara. Meanwhile, the strong influences of IOD are still found in the southern part outside of Indonesia which also occurred in September. The influences of ENSO in September are weaker than in August with a narrow distribution in the mainland area. During October, the influences of ENSO occur again in the mainland area of Indonesia, but with a lower response than in September. At the same time, the strong responses of IOD occurred in the southern part outside of Indonesia and in the centre part of Indonesia, especially in Java, Nusa Tenggara, Sulawesi, and Maluku. During November, ENSO effects begin to weaken and continue to occur until December, while the IOD effect moved slightly to the east and continue to the northeast of Indonesia in December. Influence of both climate phenomena during November is higher in the eastern part of Indonesia. The ENSO influence persists during December, whereas, at the same time, the IOD influence is not so clear in the mainland of Indonesia.

Figures 6 and 7 show the spatial patterns of monthly partial correlation between rainfalls with the two indices. Figure 6 describes the partial correlation with ENSO when the effect of IOD is removed, while Figure 7 shows the partial correlation with IOD when the effect of ENSO is removed. The partial correlations help to identify whether either or both indices should be retained for binning the monthly seasonal events. In general, ENSO and IOD are not affected by each other in all the months to influence rainfall in Indonesia. The IOD effect on ENSO in influencing rainfall occurs in January, March, June, July, October, and November, while in other months the spatial patterns are similar to the linear correlation (compare Figures 4 and 5 with Figure 6). However, the ENSO effect on IOD in influencing rainfall in Indonesia area occurs in most months, except in

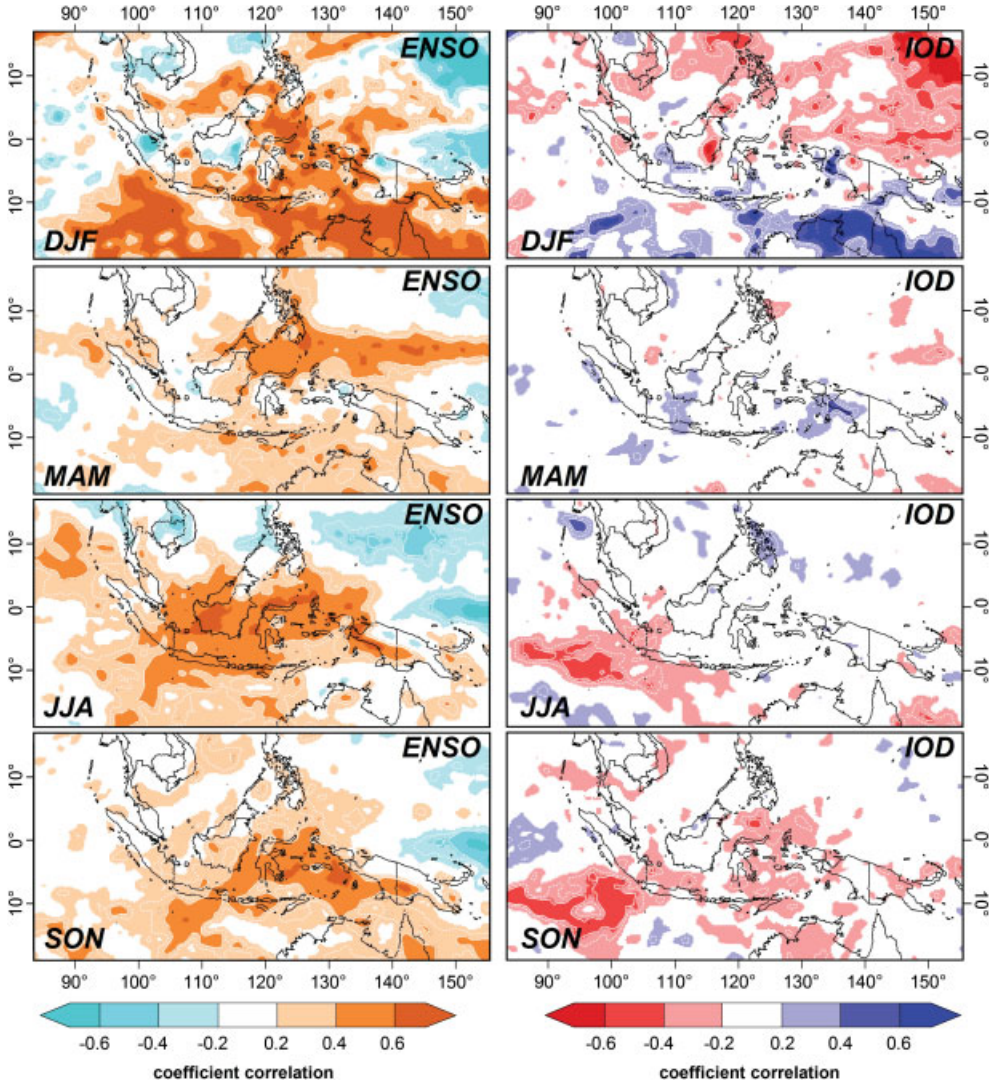

Figure 3. Seasonal patterns of spatial partial correlation between TMPA rainfall with (a) ENSO when the effect of IOD is removed and (b) IOD when the effect of ENSO is removed. White dashed line and solid line indicate significant level of correlation under 95% and 99%, respectively.

February, May, September, and December that are similar to the linear correlation (compare Figures 4 and 5 with Figure 7). The dominant influence of ENSO on rainfall in Indonesia when the effect of IOD is removed occurred in July and October, whereas that of IOD when the effect of ENSO is removed occurred in July, August, and September.

During January, March, and October, the partial correlation distributions of both climate phenomena's influence on rainfall are smaller than the liner correlation. Responses of rainfall on ENSO and IOD are disappearing in the mainland of Indonesia and reduced in the area of high partial correlation. In February, September, and December, partial correlations of both climate phenomena are similar to the linear correlation. This is shown by ENSO and IOD that are not affected by each other. Different spatial patterns have been seen in June and July, where the partial correlation of both indices is wider than the total correlation. When the effect of IOD is removed, the ENSO partial correlation distribution is wider to the south that appears to have a large degree of independence from ENSO. However, when the effect of ENSO is removed, the partial correlation of IOD has a wider spatial distribution than the total correlation. In June, the positive partial correlation occurs in the southern part of Indonesia, and in July, the partial correlation distribution occurs in the southern part of Indonesia, e.g. in Java, southern part of Sulawesi, and western part of Nusa Tenggara. The same conditions occurred in August as well where the spatial distribution of partial correlation is smaller than that in July.

4. Discussion

The spatial patterns observation of rainfall response to ENSO and IOD over Indonesia by TMPA data was explored for the period 1998–2010. Seasonal and monthly spatial linear and partial correlation analyses were done. This study proves that remote sensing data can be used to find the spatial patterns of rainfall response to

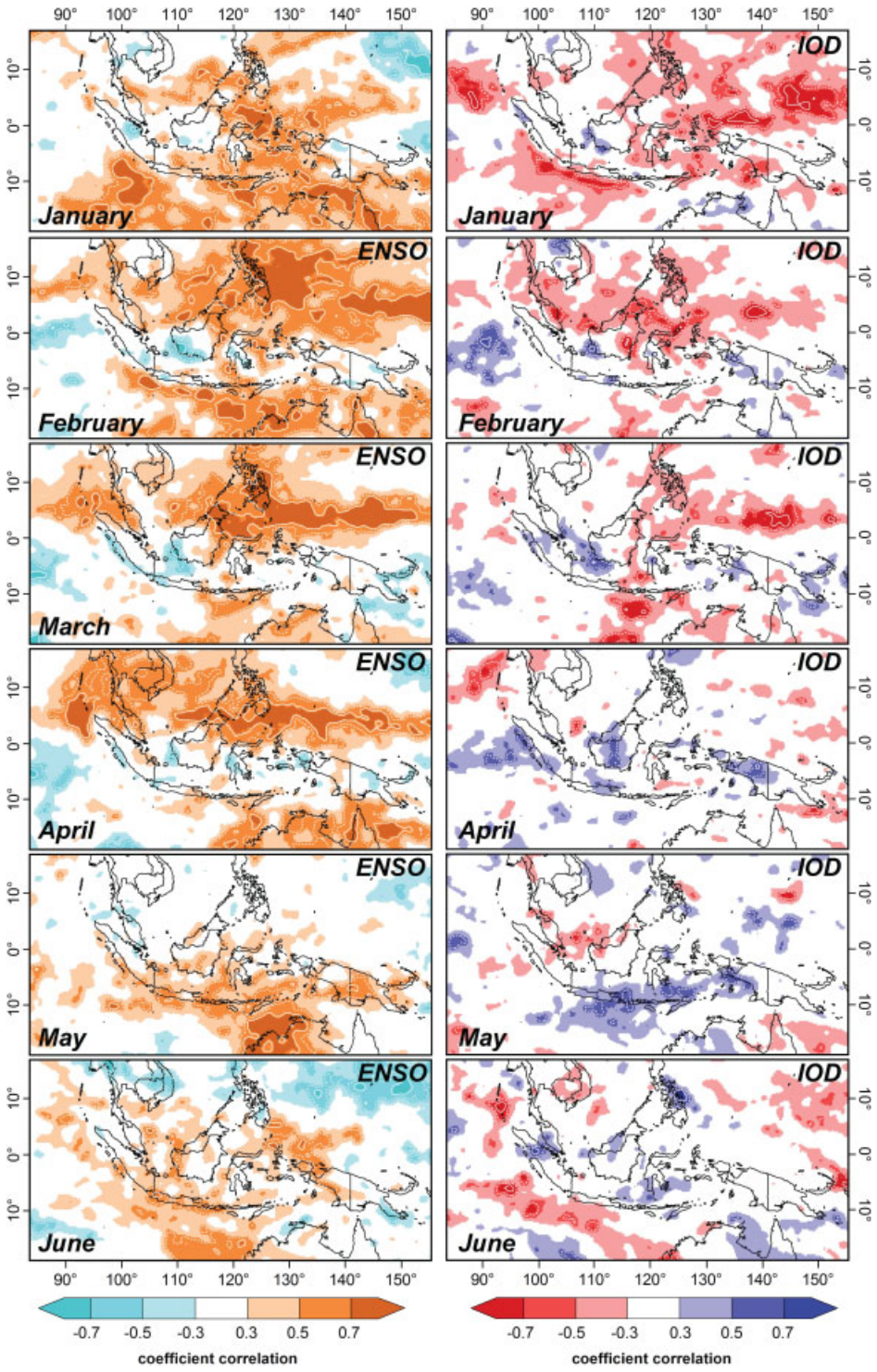

Figure 4. Monthly analysis of spatial patterns relationship between rainfall with ENSO and IOD, during January to June. White dashed line and solid line indicate significant level of correlation under 95% and 99%, respectively.

ENSO and IOD over Indonesia, where the distribution of data was quite capable of providing different information about the ENSO and IOD effects on mainland and sea.

Using the TMPA data to investigate the relationship between rainfall with ENSO and IOD has given an interesting spatial pattern. The relationship between rainfall and both indices not only describe land condition but also show spatial patterns interaction between both indices in land and sea. This phenomenon can be seen through the negative relationship between IOD and rainfall in dry season and in the beginning of rainy season (Figures 2 (g) and (h) and 5(g)–(i)) which show agglomeration relationship pattern in land and sea in the southeastern part of Java and Sumatra. The same condition is also seen through the positive spatial relationship pattern between ENSO and rainfall in MAM season

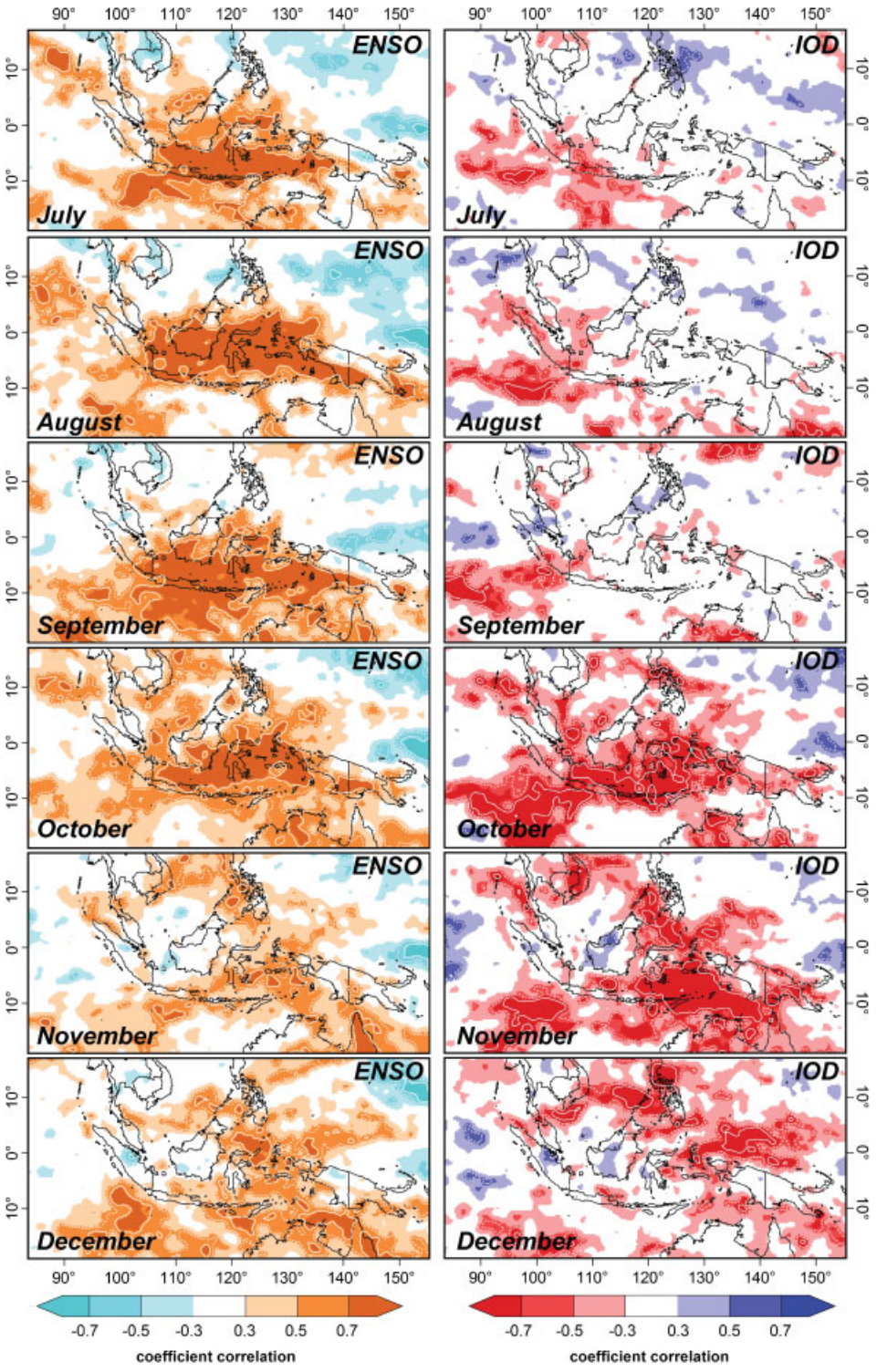

Figure 5. Same as Figure 4, but during July to December.

(Figure 2(b)), especially in March and April (Figure 4(c) and (d)). The spatial patterns distribution has shown that when most of the Indonesian land area is not correlated with ENSO, i.e. in the eastern part of Indonesia, an agglomeration positive relationship zone between ENSO and rainfall could be found from the northeast of Kalimantan, northern part of Sulawesi, and Maluku to Papua. The findings are in general agreement with Ropelewski and Halpert (1987, 1996) who state that the location of the ENSO effect occurs during October to May. On the other hand, TMPA data is not suitable to analyse the effects of local conditions on rainfall fluctuation because of low spatial resolution of the data, which is only 0.25°.

Partial correlation analysis clarified that during rainy season the spatial patterns of partial correlation are

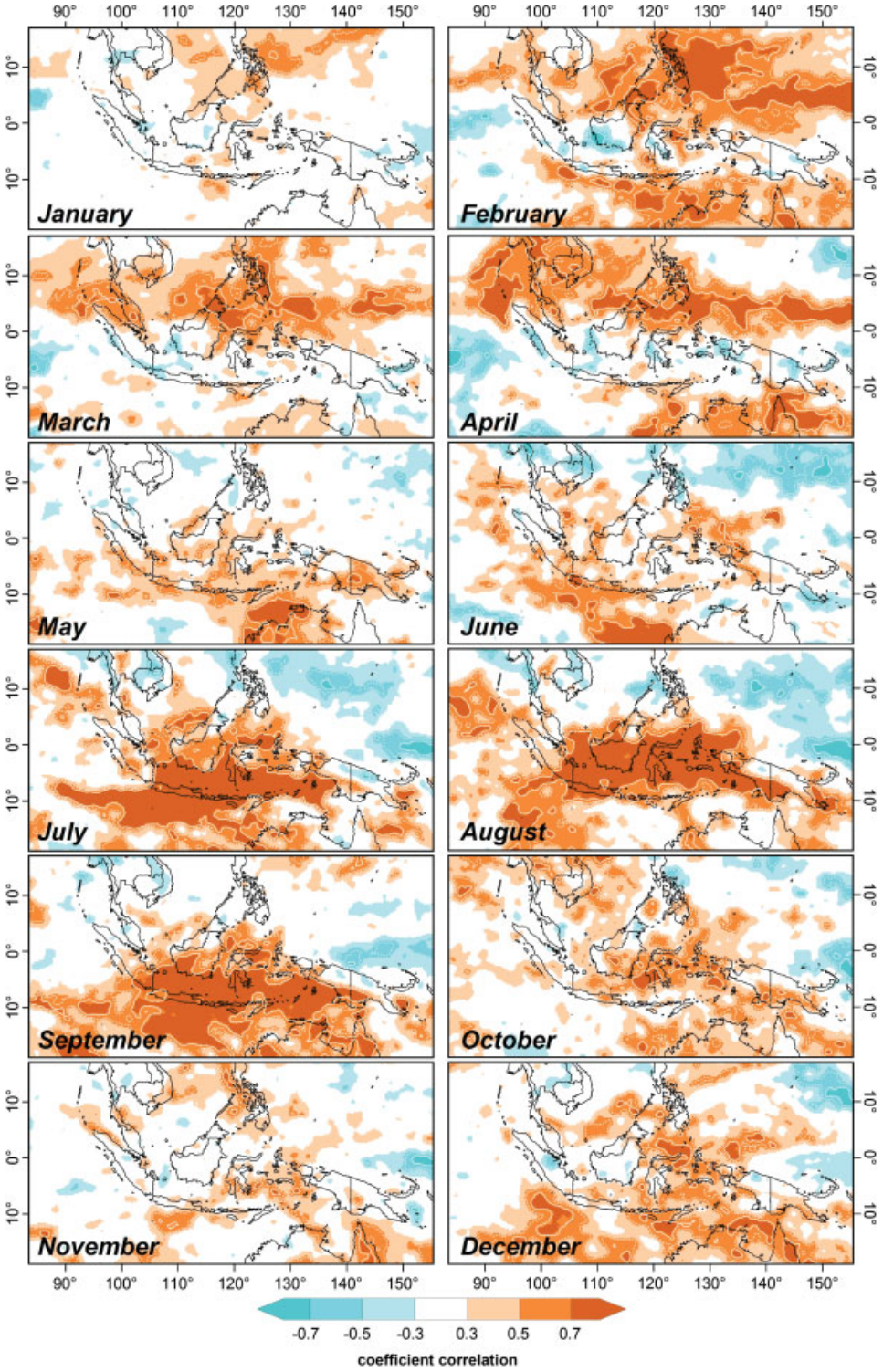

Figure 6. Spatial patterns of monthly partial correlation between TMPA with ENSO when the effect of IOD is removed. White dashed line and solid line indicate significant level of correlation under 95% and 99%, respectively.

similar to linear correlation or different from smaller ones. However, during dry season the area of partial correlation is wider than that of linear correlation. This finding informs that during rainy season the effects of both indices are uneven. In addition to this situation, there is also an interesting phenomenon in the peak dry season (June and July), during which ENSO conditions are strongly influenced by IOD, whereas the ENSO affected to IOD occur in the peak of dry season and in the beginning of rainy season.

Results of quantitative analysis show that the rainfall in Indonesia has a high relationship with ENSO and IOD, especially in dry season. Long dry season in most of the Indonesian area has a high relationship with higher SST

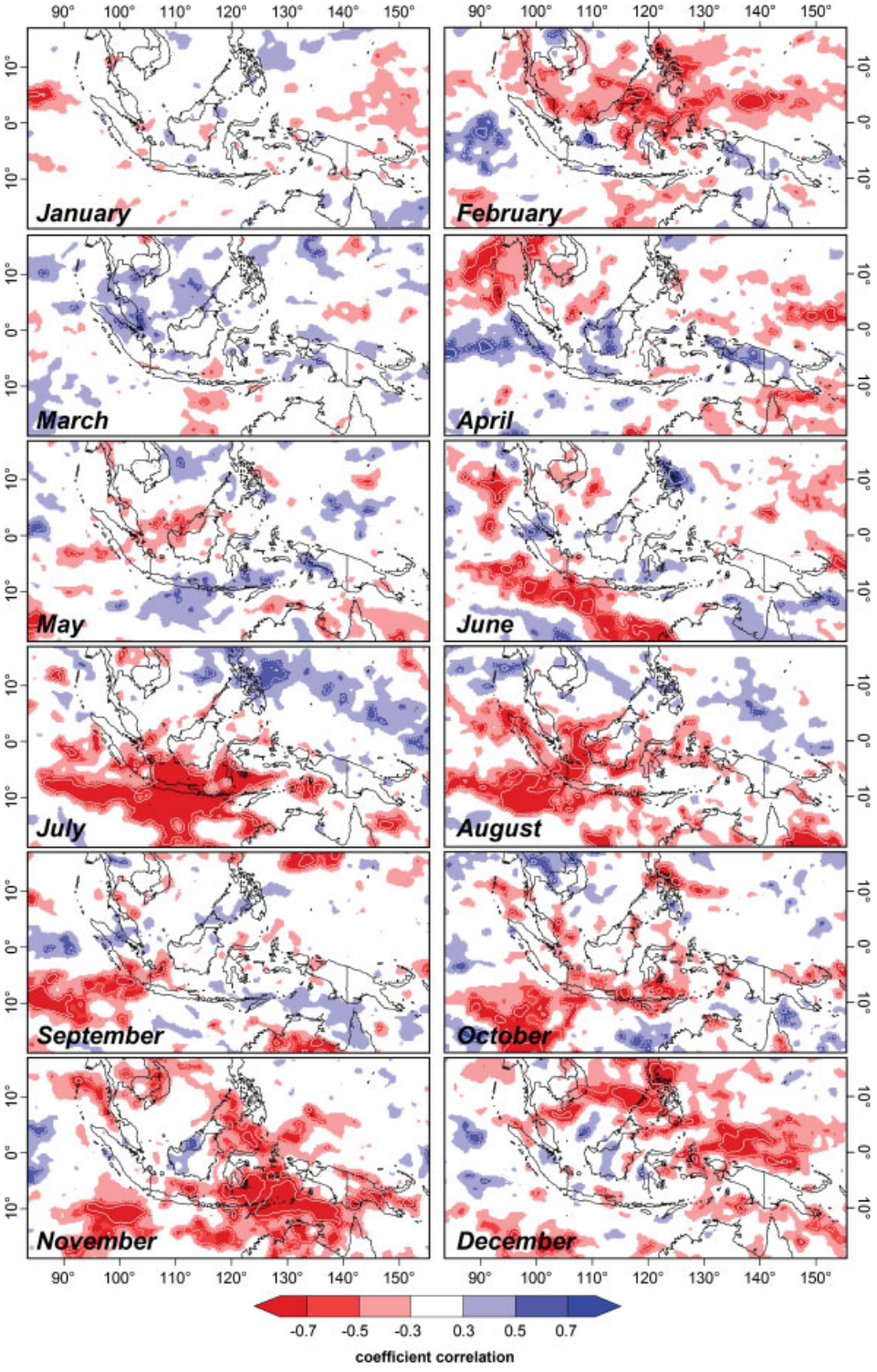

Figure 7. Same as Figure 6, but partial correlation with IOD when the effect of ENSO is removed.

in central Pacific region and lower SST in eastern Indian Ocean. On the other hand, decrease of SST in central Pacific and increase of SST in eastern Indian Ocean will cause increasing rainfall in most of the Indonesian area during dry season and advancing the rainy season. Meanwhile, during DJF season, ENSO and IOD have influenced only a small part of the Indonesian area, while during MAM monsoon season IOD does not influence rainfall and ENSO influences only a small part of Indonesia as in the DJF season. This results of this study are similar to other researches that conclude that ENSO and IOD influence rainfall in dry season, especially in August and September (e.g. Philander, 1990; Haylock and McBride, 2001; Hamada *et al.*, 2002; Aldrian and Susanto, 2003; Hendon, 2003; Saji and Yamagata, 2003b; Bannu *et al.*, 2005).

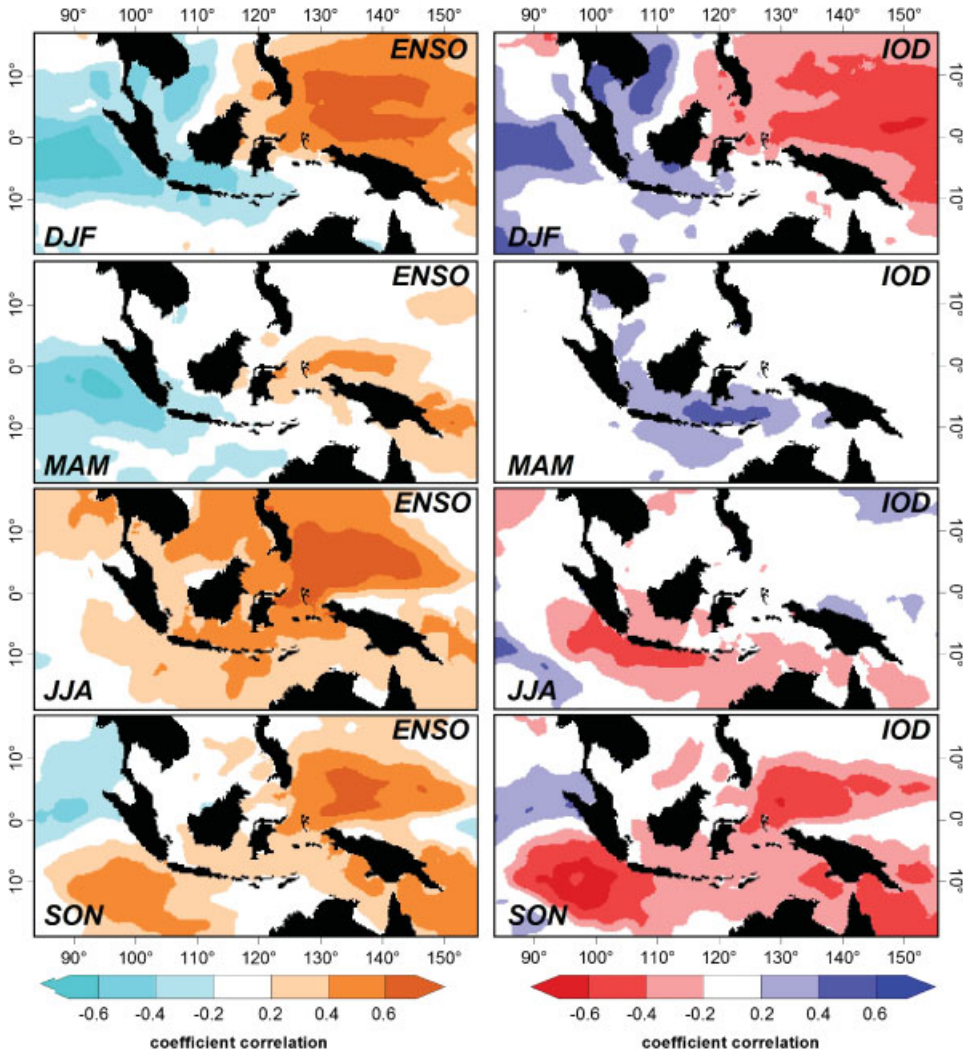

Figure 8. Seasonal analysis of the spatial patterns relationship between SST with ENSO and IOD.

High relationship between rainfall with ENSO and IOD in dry season could be a result of both those phenomena being influenced by SST in Indonesian seas and surroundings (Hendon, 2003). Further analysis on seasonal SST from TMI data through the period from 1998 to 2010 by using linear and partial correlation, respectively, are described in Figures 8 and 9. During JJA and SON seasons, the SST in inland sea of Indonesia has positive correlation with SOI and negative correlation with DMI (Figure 8(c), (d), (g), and (h)). However, for DJF and MAM, uneven correlations occur between SST and both indices in Indonesian inland sea, which ultimately affects unobvious correlations between rainfall with ENSO and IOD in rainy season (Figure 8 (a), (b), (e), and (f)). The seasonal spatial-temporal patterns of linear correlation between SST with both indices confirmed fairly similar patterns with rainfall–ENSO (rainfall–IOD) linear relationship (see Figure 2). In addition, the partial correlation analysis of SST with ENSO and IOD showed that both the phenomena interact in the peak dry season until the beginning of rainy season (Figure 9), where a similar phenomenon also occurs in partial correlation between rainfall–ENSO and rainfall–IOD (see Figure 3). These observations indicate regional and local air–sea interaction and impacted the dynamic spatial-temporal relationship between rainfalls with both indices.

Spatial relationship of SSTs with Indonesian rainfall could be explained in such aspect. During El Niño, Indonesian SST is cooler than the normal temperature. The cooler SST obstructs the evapotranspiration process which is the source of water vapour to generate rain. The opposite happens during La Niña. On the other hand, the cooler SST in Sumatra Island indicates that positive IOD also influences the evapotranspiration process in this area which causes decreasing rainfall in the surrounding area, and the opposite happens during negative IOD. The relationship of rainfall phenomena with IOD during October and November in the central part of Indonesia is an interesting subject of discussion. Generally, this is caused by the southeast monsoon from Australia and has been weakened (strengthened) because of cooler (warmer) SST in the eastern part of Indian Ocean. On the other hand, the SST in this area also causes negative

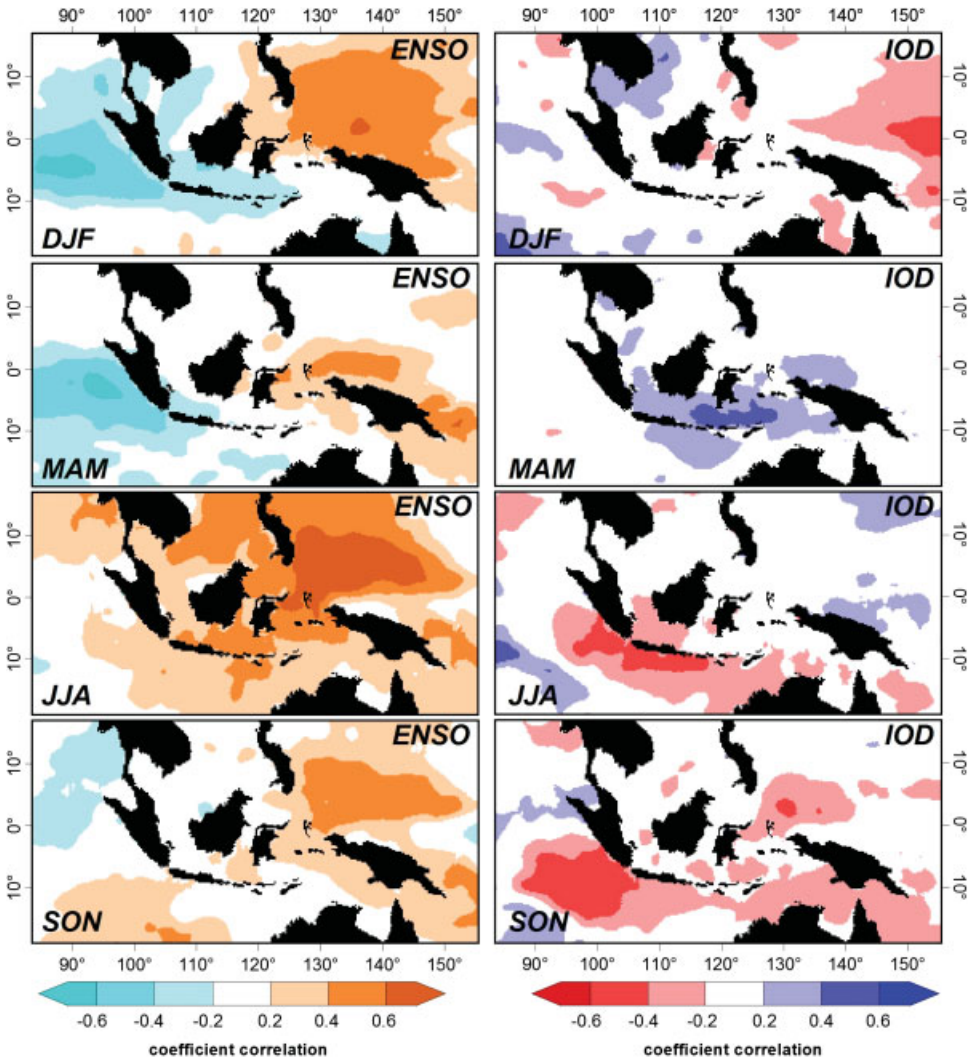

Figure 9. Seasonal patterns of spatial partial correlation between SST rainfall with (a) ENSO when the effect of IOD is removed and (b) IOD when the effect of ENSO is removed.

correlation with DMI. Cool SST anomalies lead to less evaporation and less rain, and warm SST anomalies lead to enhanced evaporation and more rain. Furthermore, they are consistent with the atmospheric circulation anomalies: more rain happens when there is anomalous surface convergence and updrafts, and less rain happens when there is anomalous surface divergence and downdrafts (Saji and Yamagata, 2003b).

The above findings show that air–sea interaction in Indonesia and its surroundings plays an important role in the difference in the ENSO and IOD strength concerning rainfall fluctuation in the spatial-temporal case. The existence of clustering distributions in ENSO and IOD affects the rain in spatial-temporal distribution, indicating that there are other effects, other than the previously described SST, which limit the ENSO and IOD effect in rainfall fluctuation in Indonesia and the surrounding area. Large clustering distributions indicate that local complex distribution of land terrain and intra-seasonal oscillation was not enough to influence the spatial-temporal clustering. However, regional and global effects may lead to a clustering zone relationship between rainfalls with both indices. For example, the existence of the Inter-Tropical Convergence Zone (ITCZ) which is the meeting area of Hedley circulation from north and south may create the clustering zone in this area. The ITCZ stripe fluctuates as a result of the movement of sun and the temperature on earth surface. The fluctuation of ITCZ and the difference in the early process during SON and MAM probably could explain in detail the reason for a strong relationship between rainfall with ENSO and IOD during SON and unclear correlation during MAM. Meanwhile, further research regarding these correlations and integration to another process with ITCZ are needed to ensure the ITCZ effect concerning spatial-temporal correlation with rainfall and ENSO and IOD in Indonesia.

5. Conclusion

Rainfall relationship spatial patterns with ENSO and IOD in Indonesia observed by TMPA, SOI, and DMI for the period 1998 to 2010 have been studied with

seasonal and monthly analysis. The results show that remote sensing data can provide good spatial-temporal clustering interactions information about the relationship between rainfall and ENSO and IOD in land and ocean area. The existence of spatial-temporal clustering zone gives the probability information on global climate which influences the difference in the ENSO and IOD strength, such as the SST and ITCZ effect.

Both ENSO and IOD have similar spatial-temporal pattern in influencing the rainfall in Indonesia. Both of those phenomena influence the rainfall fluctuation during the dry season. Meanwhile, during the rainy season, the effect is not explained clearly, especially in Indonesia. Spatial image shows that ENSO and IOD have a dynamic relationship that influences the rainfall in Indonesia. Generally, ENSO influences the rainfall fluctuation in most part of Indonesia, except the western and eastern parts. Meanwhile, IOD influences only the southern part of Indonesia especially the southeastern part of Sumatra and the western part of Java. Based on the spatial-temporal pattern that is produced, it can be concluded that the relationship between rainfall with ENSO begins in JJA, especially in July, in the southwest and central parts of Indonesia. During SON, the ENSO effect begins to move from the western part of Indonesia towards the north and a small part of south Indonesia. The ENSO effect during DJF begins to move from Indonesia towards the north and a small part of south Indonesia. Meanwhile, during MAM, especially in April, the ENSO effect moves from Indonesia and clusters to the east and southeast of Indonesia. A similar outcome also happens during the IOD phenomenon. The IOD effect begins in the southwest part of Indonesia in JJA, i.e. in July. The IOD effect begins to leave the southwest part and moves to the northeast part of Indonesia during DJF, especially in January. Also during MAM, the IOD effect moves away from Indonesia and its surrounding areas.

Acknowledgements

We gratefully acknowledge the data received from the following organizations: TMPA Satellite data from the National Aeronautics and Space Administration (NASA) Goddard Space Flight Centre (GSFC) Homepage; SOI data from the Bureau of Meteorology (BOM) Australian Government; DMI data from the Japan Agency for Marine-Earth Science and Technology (JAMSTEC); and TMI SST data from the Remote Sensing Systems (RSS) Homepage.

References

Aldrian E, Djamil YS. 2008. Spatio-temporal climatic change of rainfall in East Java Indonesia. *Int. J. Climatol.* **28**: 435–448.

Aldrian E, Susanto RD. 2003. Identification of three dominant rainfall regions within Indonesia and their relationship to sea surface temperature. *Int. J. Climatol.* **23**: 1435–1452.

Aldrian E, Gates LD, Widodo FH. 2007. Seasonal variability of Indonesian rainfall in ECHAM4 simulations and in the reanalyses: the role of ENSO. *Theor. Appl. Climatol.* **87**: 41–59.

Ashok K, Saji NH. 2007. On the impacts of ENSO and Indian Ocean Dipole events on sub-regional Indian summer monsoon rainfall. *Nat. Hazards* **42**: 273–285.

Ashok K, Nakamura H, Yamagata T. 2007. Impacts of ENSO and Indian Ocean Dipole events on the Southern Hemisphere storm-track activity during austral winter. *J. Clim.* **20**: 3147–3163.

As-syakur AR, Tanaka T, Osawa T, Mahendra MS. 2013. Indonesian rainfall variability observation using TRMM multi-satellite data. *Int. J. Remote Sens.* **34**: 7723–7738.

As-syakur AR, Tanaka T, Prasetia R, Swardika IK, Kasa IW. 2011. Comparison of TRMM Multisatellite Precipitation Analysis (TMPA) products and daily-monthly gauge data over Bali Island. *Int. J. Remote Sens.* **32**: 8969–8982.

Bannu, KH, Takeuchi N, Suriamihardja DA. 2005. Impacts of the sea surface temperature anomaly in the Pacific and Indian Oceans on the Indonesian climate. *Paper presented at the 11th CEReS International Symposium on Remote Sensing*, 13–14 December 2005, Chiba University, Chiba, Japan.

Bell GD, Halpert MS. 1998. Climate assessment for 1997. *Bull. Am. Meteorol. Soc.* **79**: S1–S50.

Bell GD, Halpert MS, Ropelewski CF, Kousky VE, Douglas AV, Schnell RC, Gelman ME. 1999. Climate assessment for 1998. *Bull. Am. Meteorol. Soc.* **80**: S1–S48.

Bell GD, Halpert MS, Schnell RC, Higgins RV, Lawrimore J, Kousky VE, Tinker R, Thiaw W, Chelliah M, Artusa A. 2000. Climate assessment for 1999. *Bull. Am. Meteorol. Soc.* **81**: S1–S50.

Blair AT. 1918. Partial correlation applied to Dakota data on weather and wheat yield. *Mon. Weather Rev.* **46**: 71–73.

Cai W, Van Rensch P, Cowan T, Hendon HH. 2011. Teleconnection pathways of ENSO and the IOD and the mechanisms for impacts on Australian rainfall. *J. Clim.* **24**: 3910–3923.

Chang C-P, Wang Z, McBride J, Liu C-H. 2005. Annual cycle of Southeast Asia – Maritime Continent rainfall and the asymmetric monsoon transition. *J. Clim.* **18**: 287–301.

Chokngamwong R, Chiu LS. 2008. Thailand daily rainfall and comparison with TRMM products. *J. Hydrometeorol.* **9**: 256–266.

Chrastansky A, Rotstayn LD. 2012. The effect of ENSO-induced rainfall and circulation changes on the direct and indirect radiative forcing from Indonesian biomass-burning aerosols. *Atmos. Chem. Phys.* **12**: 11395–11416.

Cramer D. 2003. A cautionary tale of two statistics: Partial correlation and standardised partial regression. *J. Psychol*. **137**: 507–511.

D'Arrigoa R, Wilson R. 2008. El Niño and Indian Ocean influences on Indonesian drought: implications for forecasting rainfall and crop productivity. *Int. J. Climatol.* **28**: 611–616.

Delbanco SF, Parker ML, McIntosh M, Kannel S, Hoff T, Stewart FH. 1998. Missed opportunities: teenagers and emergency contraception. *Arch. Pediatr. Adolesc. Med.* **152**: 727–733.

Feidas H. 2010. Validation of satellite rainfall products over Greece. *Theor. Appl. Climatol.* **99**: 193–216.

Fleming K, Awange JL, Kuhn M, Featherstone W. 2011. Evaluating the TRMM 3B43 monthly precipitation product using gridded raingauge data over Australia. *Aust. Meteorol. Oceanogr. J.* **61**: 171–184.

Gutman G, Csiszar I, Romanov P. 2000. Using NOAA/AVHRR products to monitor El Niño impacts: focus on Indonesia in 1997–98. *Bull. Am. Meteorol. Soc.* **81**: 1189–1205.

Hamada J-I, Yamanaka MD, Matsumoto J, Fukao S, Winarso PA, Sribimawati T. 2002. Spatial and temporal variations of the rainy season over Indonesia and their link to ENSO. *J. Meteorol. Soc. Jpn* **80**: 285–310.

Hamada J-I, Mori S, Kubota H, Yamanaka MD, Haryoko U, Lestari S, Sulistyowati R, Syamsudin F. 2012. Interannual rainfall variability over northwestern Jawa and its relation to the Indian Ocean Dipole and El Niño-Southern Oscillation events. *SOLA* **8**: 69–72.

Haylock M, McBride JL. 2001. Spatial coherence and predictability of Indonesian wet season rainfall. *J. Clim.* **14**: 3882–3887.

Hendon HH. 2003. Indonesian rainfall variability: impacts of ENSO and local air–sea interaction. *J. Clim.* **16**: 1775–1790.

Hendon HH, Wheeler MC, Zhang C. 2007. Seasonal dependence of the MJO-ENSO relationship. *J. Clim.* **20**: 531–543.

Hidayat R, Kizu S. 2010. Influence of the Madden–Julian oscillation on Indonesian rainfall variability in austral summer. *Int. J. Climatol.* **30**: 1816–1825.

Hong Y, Adler RF, Huffman GJ, Pierce H. 2010. Applications of TRMM-Based Multi-Satellite Precipitation Estimation for global runoff prediction: prototyping a global flood modelling system. In *Satellite Rainfall Applications for Surface Hydrology*, Gebremichael

M, Hossain F (eds). Springer Verlag: Dordrecht, the Netherlands; 245–266.
Huffman GJ. 1997. Estimates of root-mean-square random error for finite samples of estimated precipitation. *J. Appl. Meteorol.* **36**: 1191–1201.
Huffman GJ, Adler RF, Bolvin DT, Nelkin EJ. 2010. The TRMM Multi-satellite Precipitation Analysis (TMPA). In *Satellite Rainfall Applications for Surface Hydrology*, Gebremichael M, Hossain F (eds). Springer Verlag: Dordrecht, the Netherlands; 3–22.
Huffman GJ, Adler RF, Rudolf B, Schneider U, Keehn PR. 1995. Global precipitation estimates based on a technique for combining satellite-based estimates, rain gauge analysis, and NWP model precipitation information. *J. Clim.* **8**: 1284–1295.
Huffman GJ, Adler RF, Bolvin DT, Gu G, Nelkin EJ, Bowman KP, Hong Y, Stocker EF, Wolff DB. 2007. The TRMM Multisatellite Precipitation Analysis (TMPA): quasi-global, multiyear, combined-sensor precipitation estimates at fine scales. *J. Hydrometeorol.* **8**: 38–55.
Huffman GJ, Adler RF, Arkin P, Chang A, Ferraro R, Gruber A, Janowiak J, McNab A, Rudolph B, Schneider U. 1997. The global precipitation climatology project (GPCP) combined precipitation dataset. *Bull. Am. Meteorol. Soc.* **78**: 5–20.
Islam MN, Uyeda H. 2007. Use of TRMM in determining the climatic characteristics of rainfall over Bangladesh. *Remote Sens. Environ.* **108**: 264–276.
Irawan B. 2003. Multilevel impact assessment and coping strategies against El Niño: case of food crops in Indonesia. CGPRT Centre Working Paper No. 75, Regional Co-ordination Centre for Research and Development of Coarse Grains, Pulses, Roots and Tuber Crops in the Humid Tropics of Asia and the Pacific: United Nations, 105 p.
Kishore K, Subbiah AR. 2002. 1998–99 La Niña in Indonesia: forecasts and institutional responses. In *La Niña and Its Impacts: Facts and Speculation*, Glantz MH (ed). United Nations University Press: Tokyo, Japan; 179–185.
Können GP, Jones PD, Kaltofen MH, Allan RJ. 1998. Pre-1866 extensions of the Southern Oscillation Index using early Indonesian and Tahitian meteorological readings. *J. Clim.* **11**: 2325–2339.
Kummerow C, Simpson J, Thiele O, Barnes W, Chang ATC, Stocker E. 2000. The status of the Tropical Rainfall Measuring Mission (TRMM) after two years in orbit. *J. Appl. Meteorol.* **39**: 1965–1982.
Levizzani V, Amorati R, Meneguzzo F. 2002. A review of satellite-based rainfall estimation methods. European Commission Project MUSIC Rep. EVK1-CT-2000-00058, 66 p.
Luo J-J, Zhang R, Behera SK, Masumoto Y, Jin FF, Lukas R, Yamagata T. 2010. Interaction between El Niño and extreme Indian Ocean Dipole. *J. Clim.* **23**: 726–742.
Madden RA, Julian PR. 1971. Detection of a 40–50 day oscillation in the zonal wind in the tropical Pacific. *J. Atmos. Sci.* **28**: 702–708.
McBride JL, Haylock MR, Nicholls N. 2003. Relationships between the Maritime Continent heat source and the El Niño–Southern Oscillation phenomenon. *J. Clim.* **16**: 2905–2914.
Mehta AV, Yang S. 2008. Precipitation climatology over the Mediterranean basin from ten years of TRMM measurements. *Adv. Geosci*. **17**: 87–91.
Meyers G, McIntosh P, Pigot L, Pook M. 2007. The years of El Niño, La Niña, and interactions with the Tropical Indian Ocean. *J. Clim.* **20**: 2872–2880.
Naylor LN, Falcon WP, Rochberg D, Wada N. 2001. Using El Niño/Southern Oscillation climate data to predict rice production in Indonesia. *Clim. Change* **50**: 255–265.
Nicholls N. 1988. El Niño-Southern Oscillation and rainfall variability. *J. Clim.* **1**: 418–421.
Oh JH, Kim KY, Lim GH. 2012. Impact of MJO on the diurnal cycle of rainfall over the western Maritime Continent in the austral summer. *Clim. Dyn.* **38**: 1167–1180.
Petty GW. 1995. The status of satellite-based rainfall estimation over land. *Remote Sens. Environ.* **51**: 125–137.
Petty GW, Krajewski WF. 1996. Satellite estimation of precipitation over land. *Hydrol. Sci.* **41**: 433–451.
Philander SG. 1990. *El Niño, La Niña, and the Southern Oscillation*. Academic Press, 289 p: San Diego, CA.
Pohl B, Matthews AJ. 2007. Observed changes in the lifetime and amplitude of the Madden-Julian oscillation associated with interannual ENSO sea surface temperature anomalies. *J. Clim.* **20**: 2659–2674.
Prasetia R, As-syakur AR, Osawa T. 2013. Validation of TRMM Precipitation Radar satellite data over Indonesian region. *Theor. Appl. Climatol.* **112**: 575–587.
Qian J-H. 2008. Why precipitation is mostly concentrated over islands in the Maritime Continent. *J. Atmos. Sci.* **65**: 1428–1441.
Qian J-H, Robertson AW, Moron V. 2010. Interactions among ENSO, the monsoon, and diurnal cycle in rainfall variability over Java, Indonesia. *J. Atmos. Sci.* **67**: 3509–3524.
Rao SA, Masson S, Luo JJ, Behera SK, Yamagata T. 2007. Termination of Indian Ocean Dipole events in a coupled general circulation model. *J. Clim.* **20**: 3018–3035.
Ropelewski CF, Halpert MS. 1987. Global and regional scale precipitation patterns associated with the El Niño–Southern Oscillation. *Mon. Weather Rev.* **115**: 1606–1626.
Ropelewski CF, Halpert MS. 1989. Precipitation patterns associated with the high index phase of the Southern Oscillation. *J. Clim.* **2**: 268–284.
Ropelewski CF, Halpert MS. 1996. Quantifying Southern Oscillation–precipitation relationships. *J. Clim.* **9**: 1043–1059.
Ropelewski CF, Jones PD. 1987. An extension of the Tahiti-Darwin Southern Oscillation Index. *Mon. Weather Rev.* **115**: 2161–2165.
Sahu N, Behera SK, Yamashiki Y, Takara K, Yamagata T. 2012. IOD and ENSO impacts on the extreme stream-flows of Citarum river in Indonesia. *Clim. Dyn*. **39**: 1673–1680.
Saji NH, Yamagata T. 2003a. Structure of SST and surface wind variability during Indian Ocean Dipole Mode years: COADS observations. *J. Clim.* **16**: 2735–2751.
Saji NH, Yamagata T. 2003b. Possible impacts of Indian Ocean Dipole mode events on global climate. *Clim. Res.* **25**: 151–169.
Saji NH, Goswami BN, Vinayachandran PN, Yamagata T. 1999. A dipole mode in the tropical Indian Ocean. *Nature* **401**: 360–363.
Semire FA, Mohd-Mokhtar R, Ismail W, Norizah M, Mandeep JS. 2012. Ground validation of space-borne satellite rainfall products in Malaysia. *Adv. Space Res.* **50**: 1241–1249.
Sobel AH, Burleyson CD, Yuter SE. 2011. Rain on small tropical islands. *J. Geophys. Res.* **116**: D08102.1–D08102.15.
Susilo GE, Yamamoto K, Imai T, Ishii Y, Fukami H, Sekine M. 2013. The effect of ENSO on rainfall characteristics in the tropical peatland areas of Central Kalimantan, Indonesia. *Hydrol. Sci. J.* **58**: 539–548.
Tang Y, Yu B. 2008. MJO and its relationship to ENSO. *J. Geophys. Res.* **113**: D14106.1–D14106.18.
Trenberth KE. 1997. The definition of El Niño. *Bull. Am. Meteorol. Soc.* **78**: 2771–2777.
Vernimmen RRE, Hooijer A, Mamenun AE, van Dijk AIJM. 2012. Evaluation and bias correction of satellite rainfall data for drought monitoring in Indonesia. *Hydrol. Earth Syst. Sci.* **16**: 113–146.
von Storch H, Zwiers FW. 1999. *Statistical Analysis in Climate Research*. Cambridge University Press, 484 p: Cambridge, UK.
Waliser DE, Moncrieff MW, Burridge D, Fink AH, Gochis D, Goswami BN, Guan B, Harr P, Heming J, Hsu H-H, Jakob C, Janiga M, Johnson R, Jones S, Knippertz P, Marengo J, Nguyen H, Pope M, Serra Y, Thorncroft C, Wheeler M, Wood R, Yuter S. 2012. The "year" of tropical convection (May 2008–April 2010): climate variability and weather highlights. *Bull. Am. Meteorol. Soc.* **93**: 1189–1218.
Waple AM, Lawrimore JH. 2003. State of the climate in 2002. *Bull. Am. Meteorol. Soc.* **84**: S1–S68.
Wentz FJ, Gentemann C, Smith D, Chelton D. 2000. Satellite measurements of sea surface temperature through clouds. *Science* **288**: 847–850.
Wheeler MC, Hendon HH. 2004. An all-season real-time multivariate MJO index: development of an index for monitoring and prediction. *Mon. Weather Rev.* **132**: 1917–1932.
Wilson EA, Gordon AL, Kim D. 2013. Observations of the Madden Julian oscillation during Indian Ocean Dipole events. *J. Geophys. Res.* **118**: 2588–2599.
Xie P, Arkin PA. 1996. Analyses of global monthly precipitation using gauge observations, satellite estimates and numerical model predictions. *J. Clim.* **9**: 840–858.
Xie P, Yatagai A, Chen M, Hayasaka T, Fukushima Y, Liu C, Yang S. 2007. A gauge-based analysis of daily precipitation over East Asia. *J. Hydrometeorol.* **8**: 607–626.

